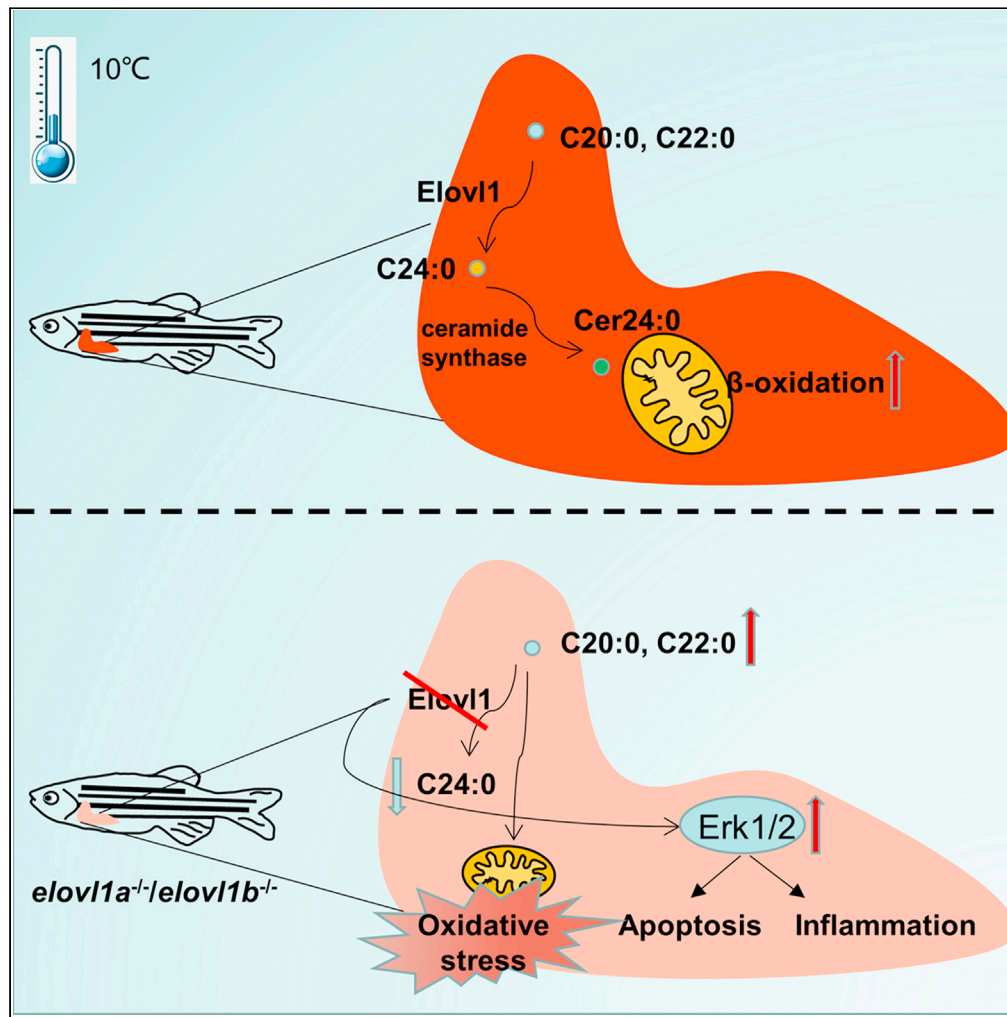**Article**

C24:0 avoids cold exposure-induced oxidative stress and fatty acid β-oxidation damage

Shouxiang Sun, Xiaojuan Cao, Jian Gao

gaojian@mail.hzau.edu.cn

Highlights

elovl1, closely associated with C24:0, was activated in ZFL cells with cold stress

C20:0 and C22:0 induced Erk1/2 expression and apoptosis to impair cold tolerance

This study showed the positive role of C24:0 in the cold resistance of fish

iScience

CellPress
OPEN ACCESS

Article

C24:0 avoids cold exposure-induced oxidative stress and fatty acid β-oxidation damage

Shouxiang Sun,[1] Xiaojuan Cao,[1,2] and Jian Gao[1,2,3,*]

SUMMARY

Low temperatures can cause severe growth inhibition and mortality in fish. Previous studies about the cold resistance of fish mainly focused on the role of unsaturated fatty acids, rather than saturated fatty acids (SFAs). In this study, the role of very-long-chain SFA synthetized by fatty acyl elongase 1 gene (*elovl1*) in cold resistance was explored. Both an aggravated liver oxidative stress and a mitochondrial metabolism disorder were observed in *elovl1a*$^{-/-}$ and *elovl1b*$^{-/-}$ zebrafish with cold stress. *In vitro* studies confirmed that high levels of C20:0 and C22:0 obviously increased the hepatocyte oxidative stress and activated the extracellular signal-regulated kinases 1/2 (Erk1/2) pathway to further induce apoptosis and inflammation. We further demonstrated that C24:0 could promote mitochondrial β-oxidation to improve the cold resistance of zebrafish. Overall, our results define a positive role of C24:0 fatty acids synthetized by *elovl1* in the cold resistance of fish.

INTRODUCTION

Fish are the largest group of poikilothermic vertebrates that cannot maintain a constant body temperature. Water temperature is one of the most important environmental factors that affect nearly all life activities of fish, including embryonic development, growth, reproduction, metabolism, and behavior (Beitinger et al., 2000; Green and Fisher, 2004; Donaldson et al., 2008). The sharp reduction of water temperature leads to significant environmental stress and seriously affects the growth and the metabolism of fish, resulting in a high mortality every year. This situation has led to large losses for many fish species around the world, both in aquaculture and wild environments (Donaldson et al., 2008; Overstreet, 1974; Wu et al., 2011). Therefore, further research in the mechanisms of cold resistance in fish, either as an economic or a research interest, is warranted.

Previous studies found that both acute and chronic cold stresses could induce mitochondrial metabolic disorder and increase the production of reactive oxygen species (ROS), which may result in oxidative stress, inflammation, and apoptosis in multiple tissues (Heise et al., 2006; Tseng et al., 2011; Vinagre et al., 2012). Excessive oxidative stress and abnormal energy metabolism are believed to be the main causes of death in fish at low temperature (Lu et al., 2019a, 2019b; Kyprianou et al., 2010). As important energy metabolic substrates, saturated fatty acids (SFAs) have been considered to promote oxidative stress and inflammation in liver tissue (Tamer et al., 2020; Rocha et al., 2016; Vogel et al., 1997). On the other hand, polyunsaturated fatty acids (PUFAs) were evidently increased in fish under cold stress to maintain the membrane stability and fluidity, which improved cold resistance (Dey et al., 1993; Buda et al., 1994; Farkas, 1980; Hazel, 1984; He et al., 2015). Hence, previous studies about the cold resistance of fish mainly focused on the role of PUFA, rather than SFA. However, it has been reported that the level of total SFA changed considerably in some fish under cold stress (Hsieh et al., 2003, 2004), of which C16:0 and C18:0 were further studied, but the very-long-chain SFAs (VLC-SFAs) were never addressed.

It has been reported that fatty acyl elongase (*Elovl*) 1, 3, and 6 are involved in the elongation of SFA (Ohno et al., 2010; Tvrdik et al., 1997; Tamura et al., 2009). *Elovl1* displays broad substrate specificities, with the ability to elongate C18-C24 SFA (Ohno et al., 2010). Researches have shown that *Elovl1* activity is regulated by ceramide synthase 2 (Cers2), which is essential for the synthesis of C24 ceramide and sphingolipid (Ohno et al., 2010; Ben-David et al., 2011; Laviad et al., 2008). Because of the teleost specific genome duplication (TSGD), teleost possesses two *elovl1* genes, namely, *elovl1a* and *elovl1b* (Bhandari et al., 2016). Previous reports indicated that *elovl1* was significantly up-regulated in fish under cold stress (Zhang et al., 2018).

[1]College of Fisheries, Key Lab of Freshwater Animal Breeding, Ministry of Agriculture, Huazhong Agricultural University, No.1 Shizishan Stress, Hongshan District, Wuhan 430070, Hubei Province, China

[2]College of Fisheries, Engineering Research Center of Green Development for Conventional Aquatic Biological Industry in the Yangtze River Economic Belt, Ministry of Education/Hubei Provincial Engineering Laboratory for Pond Aquaculture, Huazhong Agricultural University, Wuhan 430070, China

[3]Lead contact

*Correspondence: gaojian@mail.hzau.edu.cn

https://doi.org/10.1016/j.isci.2021.103409

However, it is unclear if the VLC-SFA synthetized by *elovl1* is involved in the cold resistance of fish or not, thus warranting further research.

To assess whether there was a role of VLC-SFA in the cold resistance of fish, in this study, we generated CRISPR-Cas9-mediated *elovl1a* and *elovl1b* knockout zebrafish models (namely, *elovl1a*$^{-/-}$ and *elovl1b*$^{-/-}$). We confirmed that cold stress induced an obvious change in the SFA composition of zebrafish liver (ZFL) cells. Then, we conducted a series of *in vivo* and *in vitro* experiments to determine the correlation of C24:0 synthetized by *elovl1* and cold tolerance in zebrafish. Our results showed that C24:0 played a positive role in cold resistance of fish, and C20:0 and C22:0 presented negative effects. These results enhance our understanding on the underlying mechanisms of cold resistance in fish.

RESULT
Genes *elovl1a* and *elovl1b*, closely associated with VLC-SFA, were activated in ZFL cells under cold stress

The fatty acid compositions of ZFL cells with cold stress (10°C) treatment were determined. Cold stress significantly decreased the levels of total SFA and increased the levels of total monounsaturated fatty acids (MUFAs) and PUFA (Figure 1A). Interestingly, not all SFA species levels were declined. An evident increase in the level of C24:0 in ZFL cells under cold stress was found, indicating that low temperature stimulation accelerated the synthesis of C24:0 (Figure 1B).

Figure 1C shows that the mRNA expression levels of *elovl1a* and *elovl1b* as well as levels of *Elovl1a* and *Elovl1b* were obviously increased in ZFL cells with cold stress treatment (Figure 1D). Then, the mRNA expression levels of the two genes were determined in ZFL cells treated with different SFAs (C14:0–C24:0) and MUFAs (C16:1–C22:1). The *elovl1a* expression level was significantly increased in ZFL cells incubated with C20:0, C22:0, and C24:0, compared with the control (Figure 1E). For MUFA treatment, there were no significant differences in the expression levels of *elovl1a* of ZFL cells among different treatment groups (Figure S1A). The transcription of *elovl1b* displayed 1.33-fold change (FC)- and 3.06-FC upregulation in ZFL cells treated with C20:0 and C24:0, respectively, compared with the control (Figure 1F). Meanwhile, compared with the control, *elovl1b* showed 1.26-FC and 1.49-FC upregulation in ZFL cells incubated with C20:1 and C22:1, respectively (Figure S1B).

Targeted deletion of the *elovl1a/elovl1b* caused changes in the fatty acid composition of zebrafish

We generated two mutants (*elovl1a*$^{-/-}$ and *elovl1b*$^{-/-}$ zebrafish) by using the CRISPR-Cas9 genome editing technique (Figure 2A). In this study, the target site of *elovl1a* was in the third exon. The sequencing peak map showed that *elovl1a* lacked 11 bases at the target site, resulting in the premature stop of translation at codon 66 of the Elovl1a protein (Figure 2A). The target site of *elovl1b* was in the fourth exon. The *elovl1b*$^{-/-}$ lacked 23 bases at the target site, resulting in the premature stop of translation at codon 90 of the Elovl1b protein (Figure 2A). Western blotting results showed that *elovl1a*$^{-/-}$ and *elovl1b*$^{-/-}$ zebrafish lines were successfully obtained in this study (Figure 2B). In addition, we produced a homozygous mutant of *elovl1a*$^{-/-}$*elovl1b*$^{-/-}$ (DKO) by using *elovl1a*$^{-/-}$ and *elovl1b*$^{-/-}$ zebrafish. Because the early survival rate of DKO fish was extremely low (<1%) (Figure S2A), we failed to obtain the DKO line here. In addition, a retarded growth phenotype was observed in the adult DKO (Figure S2B). There were no obvious differences in growth (Figure S2B) and the survival rate (unpublished data) between *elovl1a*$^{-/-}$/*elovl1b*$^{-/-}$ adult zebrafish and wild-type (WT) adult zebrafish.

We preliminarily explored the effects of *elovl1a/elovl1b* deletion on hepatic fatty acid compositions. Our results indicated that there were no significant differences in the total SFA, MUFA, and PUFA levels between *elovl1a*$^{-/-}$/*elovl1b*$^{-/-}$ zebrafish and WT zebrafish (Figures 2C and 2D). However, *elovl1a*$^{-/-}$ zebrafish displayed noticeably higher levels of C20:0 and C22:0 in liver tissues than WT zebrafish (Figure 2E). The contents of C20:0 and C20:1 were significantly higher in livers of *elovl1b*$^{-/-}$ zebrafish, compared with that of WT zebrafish (Figure 2F).

To fully understand the changes in hepatic lipid compositions of *elovl1a*$^{-/-}$ and *elovl1b*$^{-/-}$ zebrafish relative to WT, a hepatic lipidomic analysis was carried out. We found that *elovl1a*$^{-/-}$ and *elovl1b*$^{-/-}$ zebrafish had significantly higher levels of free fatty acid (FFA) 20:0, Cer 20:0, and sphingomyelin (SM) 20:0 and a significantly lower level of Cer 24:0, compared with WT zebrafish (Figure S3).
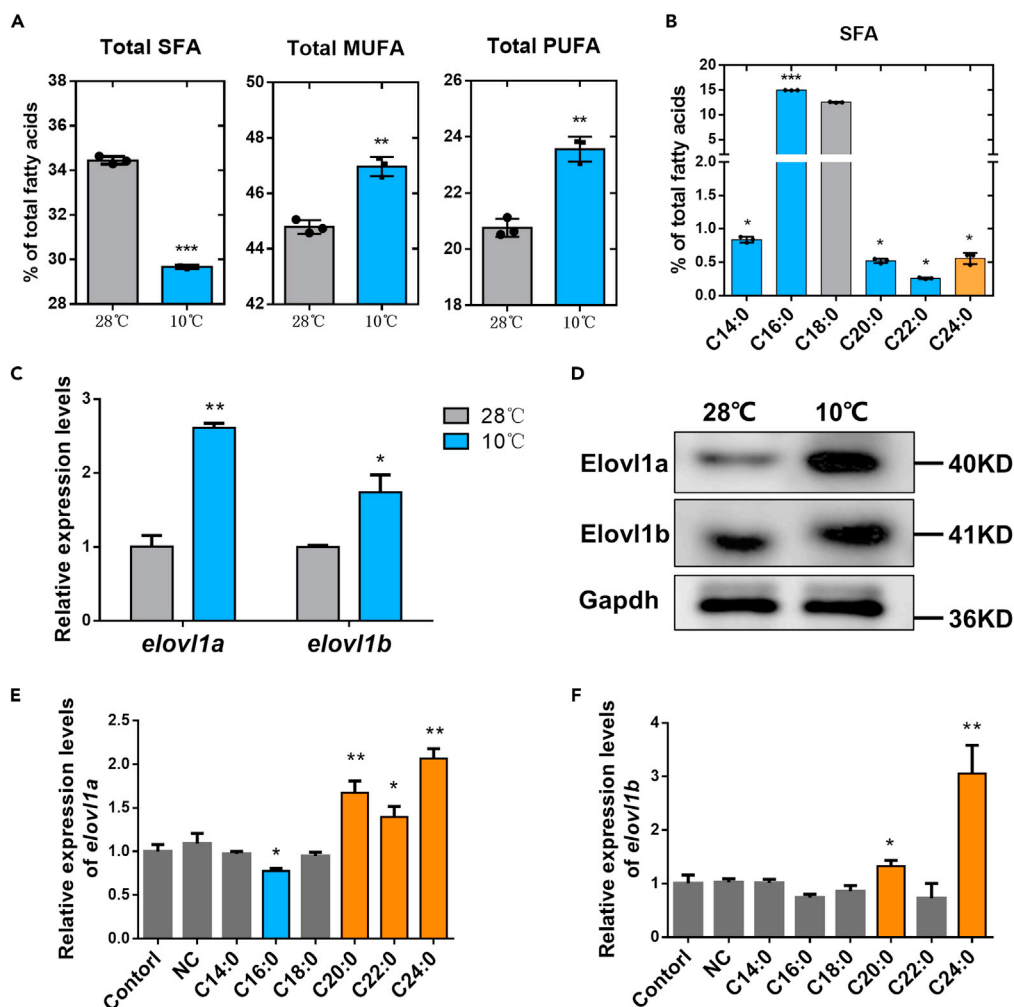
Figure 1. Fatty acid compositions and *elovl1*/Elovl1 expression levels of zebrafish liver (ZFL) cells

(A) The fatty acid compositions of ZFL cells at 28°C and 10°C.

(B) The SFA species contents of ZFL cells at 10°C.

(C) The mRNA expression levels of *elovl1a* and *elovl1b* in ZFL cells at 28°C and 10°C.

(D) The protein expression levels of Elovl1a and Elovl1b in ZFL cells at 28°C and 10°C.

(E and F) The expression levels of *elovl1a* (E) and *elovl1b* (F) in control and SFA-treatment ZFL cells at 28°C. The blue and orange colors in (B), (E), and (F), respectively, meant significant decrease and increase in parameters of treated groups, compared with the control (the control in (B) was the SFA species content of ZFL cells at 28°C). Data were given as means ± SD of three biological replicates. The statistical analyses were conducted by t test. The asterisks labeled above the error bars indicated significant differences (*p < 0.05, **p < 0.01, ***p < 0.001). SFA, saturated fatty acid; MUFA, monounsaturated fatty acid; PUFA, polyunsaturated fatty acid; NC, negative control; elovl1, fatty acyl elongase 1; Gapdh, glyceraldehyde-3-phosphate dehydrogenase.

Deletion of *elovl1a*/*elovl1b* impairs the cold resistance of zebrafish

To determine the role of Elovl1s in cold stress, we exposed WT, *elovl1a*^{−/−}, and *elovl1b*^{−/−} zebrafish to cold stress. The fatty acid compositions of livers in WT, *elovl1a*^{−/−}, and *elovl1b*^{−/−} zebrafish were measured. The *elovl1a*^{−/−} and *elovl1b*^{−/−} zebrafish presented significantly higher levels of C20:0 and lower levels of C24:0 than WT zebrafish (Figures S4A and S4B). We found that *elovl1a*/*elovl1b* deletion significantly lowered the survival rate of zebrafish exposed to cold stress (Figure 3A). All *elovl1a*^{−/−} zebrafish died after 180 h of cold stress. Under cold stress, liver tissues of *elovl1a*^{−/−} and *elovl1b*^{−/−} zebrafish were paler compared with that of WT zebrafish (Figure S4C). The pathological sections of livers further indicated that cold stress caused liver damage in *elovl1a*^{−/−} and *elovl1b*^{−/−} zebrafish. The number of lymphocytes, markers of inflammatory infiltration, was obviously increased in liver tissues of *elovl1a*^{−/−} and *elovl1b*^{−/−} zebrafish (Figure 3B).
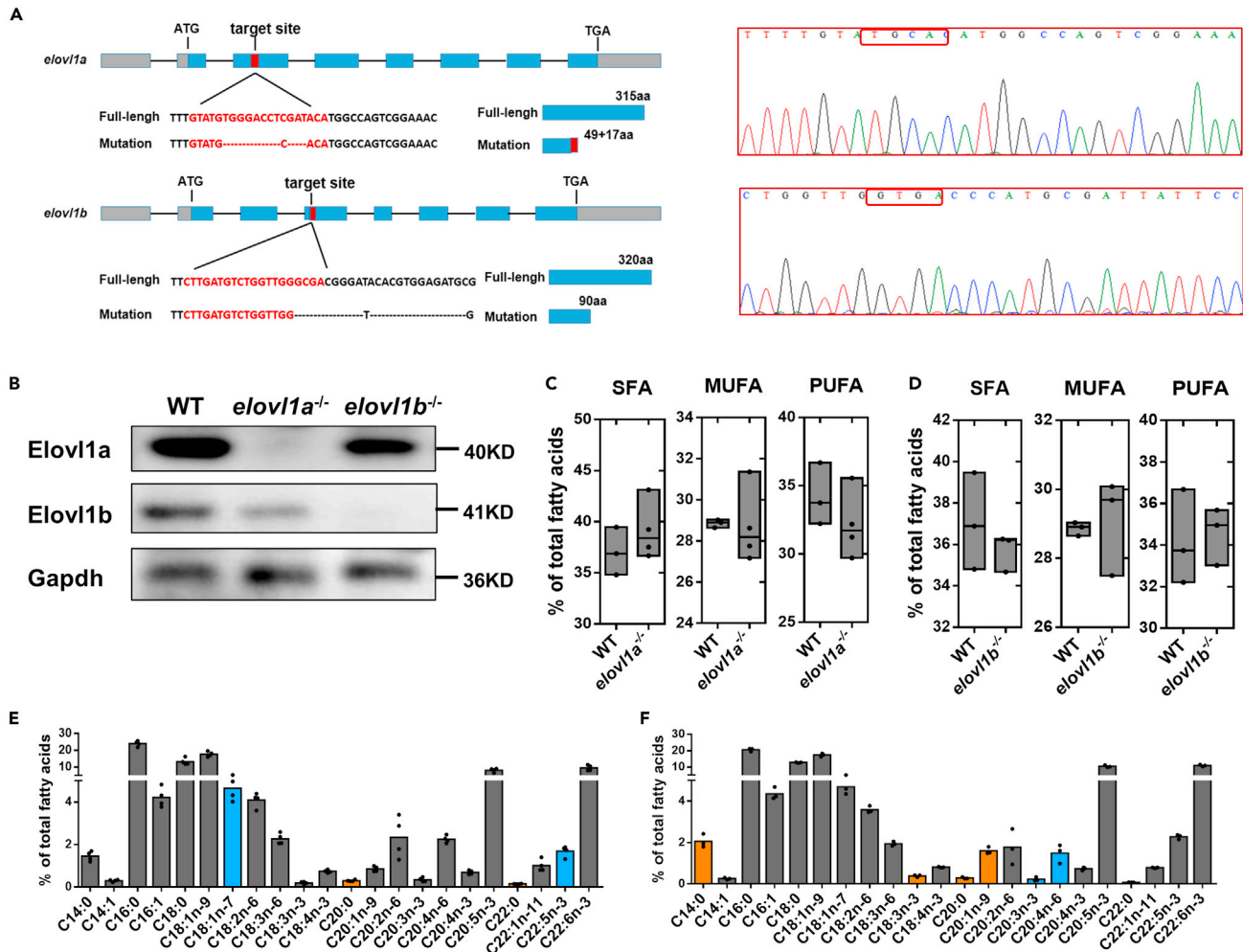
Figure 2. Deletion of *elovl1a* and *elovl1b* genes in zebrafish and their effects on fatty acid compositions

(A) The targeting site for *elovl1a* and e*lovl1b* gene knockout. The gray boxes were the 5′-untranslated and 3′-untranslated regions, and blue boxes the exons. The red boxes indicated the targeting sequences.

(B) Mutation confirmation, as shown by the results of the protein expression of Elovl1a and Elovl1b.

(C and D) The total SFA, MUFA, and PUFA contents in livers of 2-month-old WT, *elovl1a*$^{-/-}$ (C) and *elovl1b*$^{-/-}$ (D) zebrafish.

(E and F) Fatty acid compositions in livers of 2-month-old *elovl1a*$^{-/-}$ (E) and *elovl1b*$^{-/-}$ (F) zebrafish. The blue and orange colors in (E) and (F), respectively, meant significant decrease and increase in parameters of *elovl1a*$^{-/-}$/*elovl1b*$^{-/-}$ zebrafish, compared with WT zebrafish ($p < 0.05$). Data were given as means ± SD of three or four biological replicates. The statistical analyses were conducted by t test. WT, wild-type zebrafish; elovl1, fatty acyl elongase 1; *elovl1a*$^{-/-}$, *elovl1a* knockout zebrafish; *elovl1b*$^{-/-}$, *elovl1b* knockout zebrafish; SFA, saturated fatty acid; MUFA, monounsaturated fatty acid; PUFA, polyunsaturated fatty acid; Gapdh, glyceraldehyde-3-phosphate dehydrogenase.

Next, we determined the oxidative stress level of liver tissues by measuring malondialdehyde (MDA) level and catalase (CAT) activity. As shown in Figure 3C, the MDA levels were significantly increased in liver tissues of *elovl1a*$^{-/-}$ and *elovl1b*$^{-/-}$ zebrafish under cold stress, compared with WT zebrafish (Figure 3C). The CAT activities in livers of *elovl1a*$^{-/-}$ and *elovl1b*$^{-/-}$ zebrafish were significantly decreased (Figure 3D). The deletion of *elovl1a* or *elovl1b* obviously reduced the mRNA expression levels of antioxidant stress-related genes, including glutathione peroxidase 1a (*gpx1a*), *gpx1b*, superoxide dismutase 1 (*sod1*), and catalase 1 (*cat1*) in zebrafish under cold stress (Figure 3E), but there were no significant differences in the expression levels of these genes between *elovl1a*$^{-/-}$/*elovl1b*$^{-/-}$ and WT zebrafish at 28°C (Figure S4D). Thus, it indicated that *elovl1a*$^{-/-}$ and *elovl1b*$^{-/-}$ zebrafish under cold stress had more severe oxidative stress, which caused liver tissue damages.

Tissue damage is always accompanied by apoptosis and inflammation (Davidovich et al., 2014; Busch et al., 2012). The up-regulated expression levels of apoptosis and inflammation-related genes were also
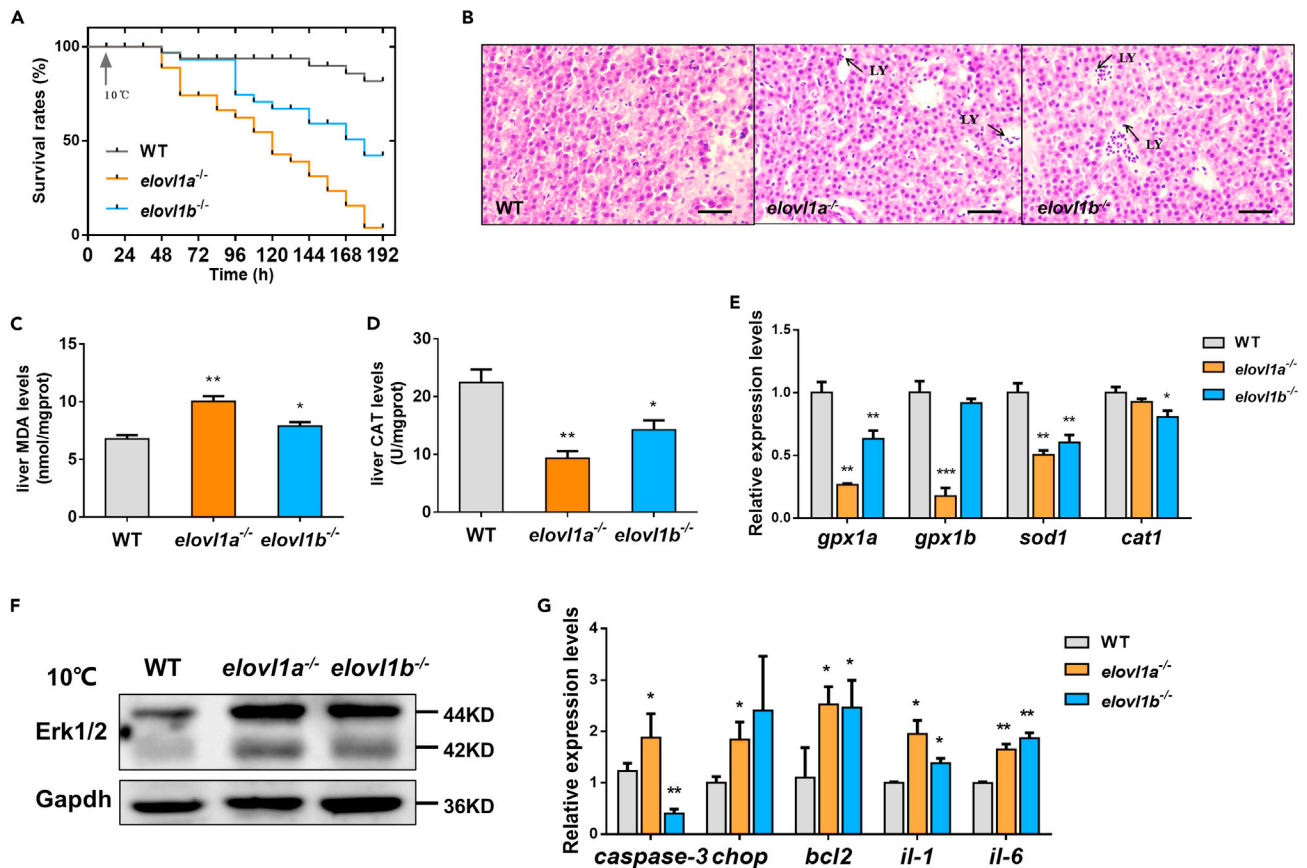
Figure 3. Effects of *elovl1a* and *elovl1b* deletion on cold tolerance of zebrafish

(A) The survival rates of fish during cold stress.

(B) Histological structures of livers from WT, *elovl1a*$^{-/-}$, and *elovl1b*$^{-/-}$ zebrafish under cold stress. Scale bar, 20 μm.

(C and D) The levels of MDA (C) and CAT (D) in livers of WT, *elovl1a*$^{-/-}$, and *elovl1b*$^{-/-}$ zebrafish under cold stress (n = 5).

(E) Hepatic expression levels of four oxidative stress-related genes in WT, *elovl1a*$^{-/-}$, and *elovl1b*$^{-/-}$ zebrafish under cold stress.

(F) Western blotting of Erk1/2 in livers of WT, *elovl1a*$^{-/-}$, and *elovl1b*$^{-/-}$ zebrafish under cold stress.

(G) Hepatic expression levels of apoptosis and inflammation-related genes in WT, *elovl1a*$^{-/-}$, and *elovl1b*$^{-/-}$ zebrafish under cold stress. Data were given as means ± SD of three biological replicates unless otherwise specified. The statistical analyses were conducted by t test. The asterisks labeled above the error bars indicated significant differences (*$p < 0.05$, **$p < 0.01$, ***$p < 0.001$). WT, wild-type zebrafish; elovl1, fatty acyl elongase 1; *elovl1a*$^{-/-}$, *elovl1a* knockout zebrafish; *elovl1b*$^{-/-}$, *elovl1b* knockout zebrafish; LY, lymphocyte; MDA, malondialdehyde; CAT, catalase; *gpx-1a*, glutathione peroxidase 1a; *sod1*, superoxide dismutase 1, soluble; *cat1*, catalase 1; Erk1/2, extracellular signal-regulated kinases 1/2; Gapdh, glyceraldehyde-3-phosphate dehydrogenase; *chop*, DNA damage inducible transcript 3; *bcl2*, BCL2 apoptosis regulator a; *il*, interleukin.

important indicators of tissue damages. A number of studies have demonstrated that cold stress causes the activation of extracellular signal-regulated kinases 1/2 (Erk1/2), major components of the greater mitogen-activated protein kinase (Mapk) cascade, which has been connected with increased inflammation and apoptosis (Sabnam and Pal, 2019; Sun et al., 2020a, 2020b). In this study, notable increases in Erk1/2 expression levels were found in *elovl1a*$^{-/-}$ and *elovl1b*$^{-/-}$ zebrafish under cold stress, compared with WT zebrafish (Figure 3F). At 28°C, *elovl1a*$^{-/-}$/*elovl1b*$^{-/-}$ zebrafish (relative to WT) exhibited no significant differences in the expression levels of apoptosis-related genes (including *caspase-3*, DNA-damage-inducible transcript 3 [*chop*], and BCL2 apoptosis regulator a [*bcl2*]) and inflammation-related genes (interleukin-1 [*il-1*], *il-6*) (Figure S4E). However, almost all these genes (except *caspase-3* in *elovl1b*$^{-/-}$ zebrafish) were up-regulated in *elovl1a*$^{-/-}$/*elovl1b*$^{-/-}$ zebrafish under cold stress, compared with WT zebrafish (Figure 3G). Lipid catabolism, especially fatty acid β-oxidation, plays an important role in the cold resistance (Lu et al., 2019b). Three mitochondrial β-oxidation-related genes (*peroxisome proliferator-activated receptor gamma, coactivator 1 alpha* [*pgc-1a*], carnitine palmitoyltransferase 1a [*cpt-1a*], and ATP synthase F1 subunit beta [*atp5b*]) were significantly down-regulated in *elovl1a*$^{-/-}$/*elovl1b*$^{-/-}$ zebrafish compared with WT zebrafish under cold stress (Figure S4F).

The accumulation of C20:0 and C22:0 damaged the cold tolerance of ZFL cells, whereas C24:0 promoted β-oxidation via ceramide synthetase to improve the cold tolerance.

To further identify the roles of different SFAs in the cold resistance, *in vitro* experiments were performed. ZFL cells were incubated with C18:0 (5 μM), C20:0 (5 μM), C22:0 (5 μM), and C24:0 (5 μM). The results of fatty acid compositions of ZFL cells confirmed that the incubation of SFA was successful (Figure S5A). The 5-μM SFA treatment did not affect the growth of ZFL cells at 28°C (Figure S5B). Under cold stress, the apoptotic level was significantly increased in ZFL cells incubated with C20:0 or C22:0 and significantly decreased in cells incubated with C24:0 compared with control (Figure 4A). Moreover, the expression of Erk1/2 and two apoptosis-related genes (*caspase-3* and *chop*) was up-regulated in ZFL cells incubated with C20:0 and C22:0 (Figures 4B and 4C). On the contrary, C24:0 treatment alleviated the Erk1/2 expression, compared with the control (Figure 4B). In addition, the increased apoptosis level and up-regulated Erk1/2 expression induced by C20:0 or C22:0 treatment can be counteracted by VE (a typical antioxidant) treatment under cold stress (Figures 4D and 4E).

C24:0 ceramide has been reported to be localized in the mitochondrial membrane and promotes the mitochondrial β-oxidation process (Raichur et al., 2014; Mesicek et al., 2010). It is noteworthy that the mRNA expression levels of C24:0 ceramide synthetase-related genes (*cers2a*, *cers2b*, and *cers4b*) were significantly higher in ZFL cells treated with C24:0, compared with the control (Figure 4F). Meanwhile, the C16:0 ceramide synthetase-related gene (*cers6*, Turpin et al., 2014) was significantly down-regulated in ZFL cells treated with C24:0. C24:0 treatment significantly increased the mRNA expression levels of mitochondrion β-oxidation-related genes (*pgc-1a*, *cpt-1a*, and *atp5b*) under cold stress (Figure 4G).

SFA diet feeding trial verified that C24:0 played a positive role in the cold resistance of zebrafish

To verify the effect of SFA on the cold tolerance of zebrafish, we conducted a feeding experiment *in vivo*. The C20:0 and C22:0 diet feeding obviously decreased the survival rate of zebrafish exposed to cold stress. Compared with the control, the zebrafish fed with C24:0 diet had a lower mortality (Figure S6). We found paler liver tissues in zebrafish fed with enriched C20:0 or C22:0 diet when compared with control and C24:0 diet group under cold stress (Figure 5A). Under cold stress, the fish fed with C20:0 and C22:0 diet had increased hepatic MDA levels and decreased hepatic CAT activities (Figures 5B and 5C). Compared with the control, the expression of Erk1/2 was up-regulated in livers from the C20:0 diet group under cold stress (Figure 5D). Moreover, the expression levels of *chop* and *il-1* in livers from C20:0 and C22:0 diet groups were significantly higher than those in the control and C24:0 diet group (Figure 5E). The expression levels of ceramide synthetase-related genes such as *cers6*, *cers2a*, *cers2b*, and *cers4b* were investigated (Figures 5F and 5G). Compared with control, *cers6* was significantly up-regulated in livers from the C18:0 diet group, whereas the opposite was observed in the C24:0 diet group (Figure 5F). Higher expression levels of C24:0 ceramide synthetase-related genes (*cers2a*, *cers2b*, and *cers4b*) and mitochondrial β-oxidation-related genes (*pgc-1a*, *cpt-1a*, and *atp5b*) were detected in the C24:0 diet group compared with the control group (Figures 5G and 5H).

DISCUSSION

So far, unlike PUFAs, SFAs have received limited attention on their potential impacts on the cold resistance of fish. This study shows that the level of total SFAs was significantly decreased in ZFL cells under cold stress. Interestingly, when C14-C22 SFA contents obviously decreased, the content of C24:0 was significantly increased, indicating that cold stress promoted the synthesis of VLC-SFA (namely, C24:0) in zebrafish. Therefore, it suggested that C24:0 would involve in cold adaption in fish and play different functions from C14 to C22 SFAs.

The genes *elovl1a* and *elovl1b* were reported to be involved in the elongation of SFAs from C18 to C24 (Ohno et al., 2010). Our results showed that the expressions of these two genes were activated in ZFL cells under cold stress. In addition, the expressions of *elovl1a* and *elovl1b* were more susceptible in ZFL cells incubated with C20:0 and C24:0. Moreover, the deletion of *elovl1a/elovl1b* resulted in the accumulation of C20:0. Thus, the *elovl1a$^{-/-}$* and *elovl1b$^{-/-}$* zebrafish could be good models to study the effects of SFA composition on the cold resistance of fish.
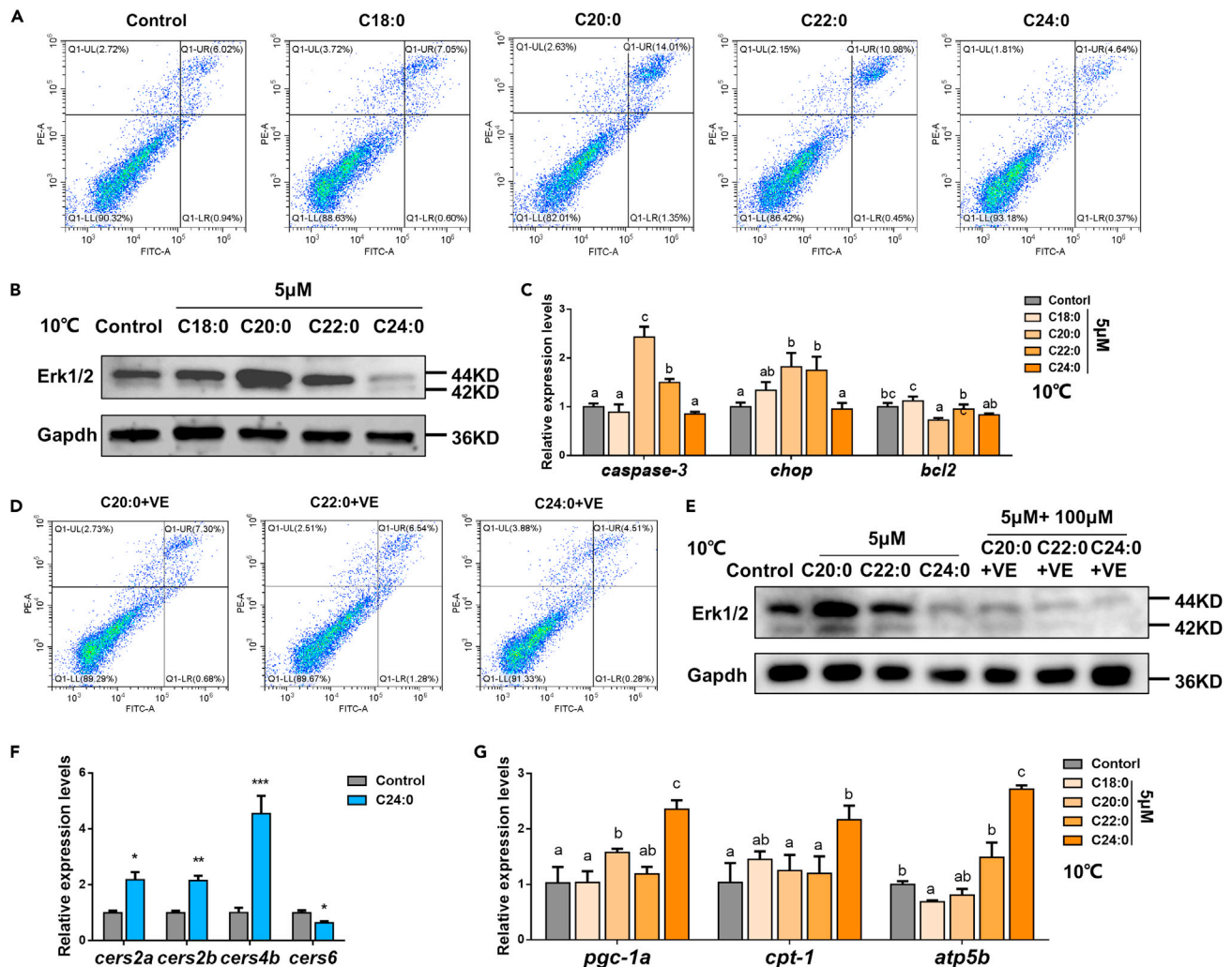
Figure 4. Effects of different saturated fatty acids (SFA, C18–C24) on cold tolerance of zebrafish liver (ZFL) cells

(A) Apoptotic levels of ZFL cells under cold stress, after incubation with different SFAs.

(B) Western blotting of Erk1/2 in ZFL cells under cold stress, after incubation with different SFAs.

(C) The expression levels of apoptosis-related genes in ZFL cells under cold stress, after incubation with different SFAs.

(D) Apoptotic levels of ZFL cells under cold stress, after incubation with different SFAs + VE.

(E) Western blotting of Erk1/2 in ZFL cells under cold stress, after incubation with different SFAs + VE.

(F) The expression levels of four ceramide synthase genes in ZFL cells under cold stress, after incubation with C24:0.

(G) The expression levels of β-oxidation-related genes in ZFL cells under cold stress, after incubation with different SFAs. Data were given as means ± SD of three biological replicates. The statistical analyses were conducted by t test or one-way ANOVA with Tukey's post hoc test. The different letters above the bars indicated significant differences ($p < 0.05$). The asterisks labeled above the error bars indicated significant differences (*$p < 0.05$, **$p < 0.01$, ***$p < 0.001$). Erk1/2, extracellular signal-regulated kinases 1/2; Gapdh, glyceraldehyde-3-phosphate dehydrogenase; *chop*, DNA damage inducible transcript 3; *bcl2*, BCL2 apoptosis regulator a; VE, vitamin E; *cers*, ceramide synthase; *pgc-1a*, peroxisome proliferator-activated receptor-γ coactivator-1a; *cpt-1a*, carnitine palmitoyl transferase 1a; *atp5b*, ATP synthase F1 subunit beta.

In this study, we found that the deletion of *elovl1a*/*elovl1b* impaired the ability of cold resistance in zebrafish, which was manifested by increased levels of apoptosis, inflammation, and oxidative stress. Erk1/2 expression was found to be activated in *elovl1a*$^{-/-}$ and *elovl1b*$^{-/-}$ zebrafish. Previous studies have shown that cold-stress-induced cell death involves the activation of the Erk1/2 pathway (Patterson et al., 2009; Kondoh and Nishida, 2007). The ROS-induced oxidative stress is considered to be a potential factor for the activation of the Erk1/2 pathway. SFAs produce more ROS than unsaturated fatty acids during β-oxidation (Plötz et al., 2019). The reduction of the toxicity was as more pronounced as more proximal the double bond was positioned to the carbonyl group, since this reduced the number of undisturbed cycles in the
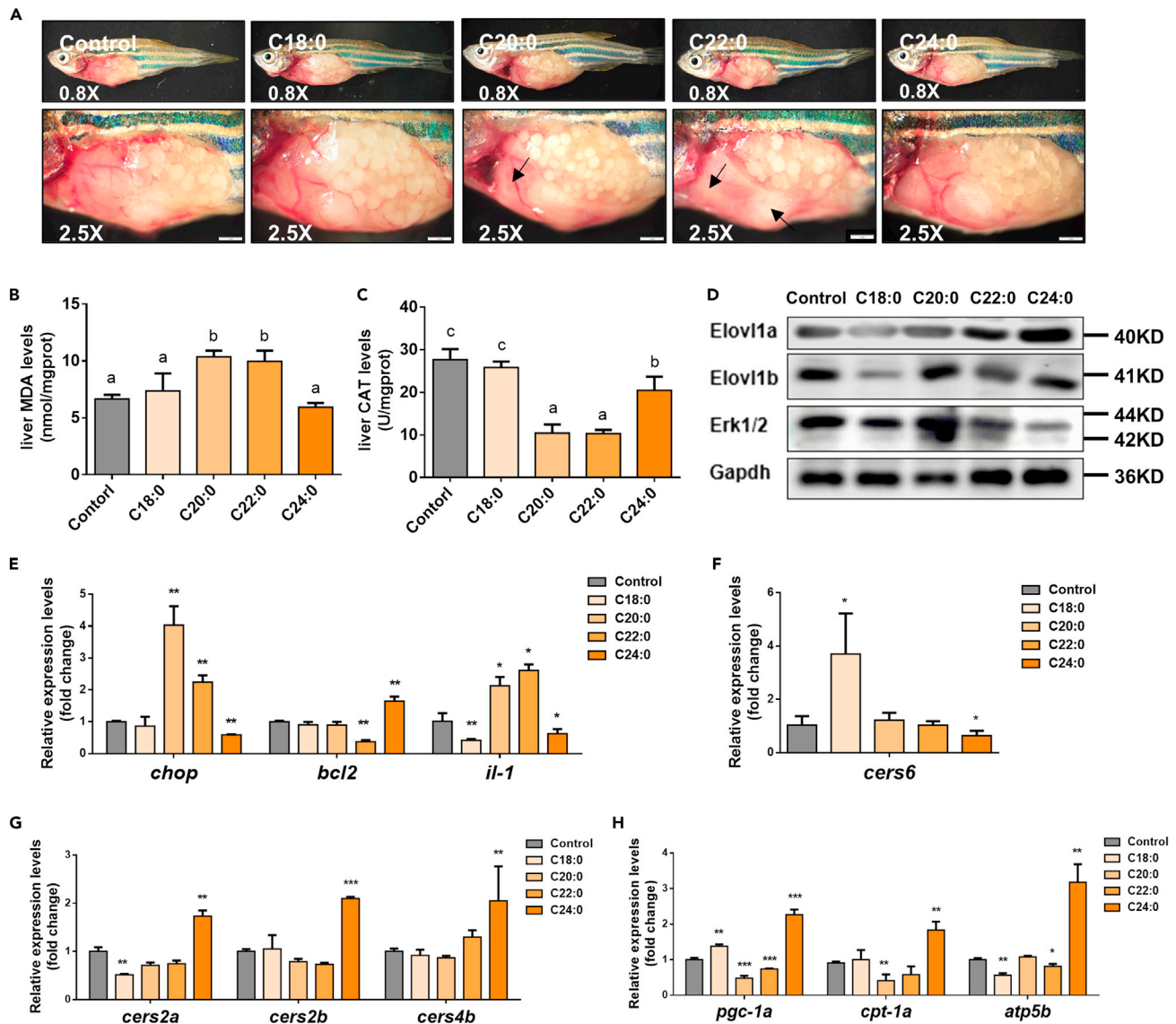
Figure 5. Effects of different dietary saturated fatty acids (SFA) on cold tolerance of zebrafish

(A) The liver lesions of zebrafish under cold stress, after being fed with different SFA diets for 2 weeks. Scale bar, 1 mm.

(B and C) The levels of hepatic MDA (B) and CAT (C) in zebrafish under cold stress, after being fed with different SFA diets for 2 weeks.

(D) Western blotting of Elovl1a, Elovl1b, and Erk1/2 in livers of zebrafish under cold stress, after being fed with different SFA diets for 2 weeks.

(E) Hepatic expression levels of apoptosis and inflammation-related genes in zebrafish under cold stress, after being fed with different SFA diets for 2 weeks.

(F and G) The expression levels of four ceramide synthase genes in livers of zebrafish under cold stress, after being fed with different SFA diets for 2 weeks.

(H) The expression levels of β-oxidation-related genes in livers of zebrafish under cold stress, after being fed with different SFA diets for 2 weeks. Data were given as means ± SD of three biological replicates. The statistical analyses were conducted by t test or one-way ANOVA with Tukey's post hoc test. The different letters above the bars indicated significant differences ($p < 0.05$). The asterisks labeled above the error bars indicated significant differences (*$p < 0.05$, **$p < 0.01$, ***$p < 0.001$). MDA, malondialdehyde; CAT, catalase; Elovl1, fatty acyl elongase 1; Erk1/2, extracellular signal-regulated kinases 1/2; Gapdh, glyceraldehyde-3-phosphate dehydrogenase; *chop*, DNA damage inducible transcript 3; *bcl2*, BCL2 apoptosis regulator a; *il*, interleukin; *cers*, ceramide synthase; *pgc-1a*, peroxisome proliferator-activated receptor-γ coactivator-1a; *cpt-1a*, carnitine palmitoyl transferase 1a; *atp5b*, ATP synthase F1 subunit beta.

β-oxidation spiral (Kunau et al., 1995; Schulz, 1994). This cytotoxicity is characterized by the activation of apoptosis (Šrámek et al., 2017; Plötz et al., 2019). Previous reports indicated that C20:0 had the highest lipotoxicity compared with PUFAs and other SFAs (Plötz et al., 2019). The C20:0 accumulated in livers of *elovl1a⁻/⁻* and *elovl1b⁻/⁻* zebrafish. Therefore, it is reasonable to speculate that the weakening of cold

resistance ability in $elovl1a^{-/-}/elovl1b^{-/-}$ zebrafish may be attributed to the metabolic disorder of SFA, especially C20:0. In addition, the results of *in vitro* experiments showed that C20:0 or C22:0 incubation increased the apoptotic levels of ZFL cells under cold stress, which was in line with the *in vivo* experiment results.

Lipid droplet formation has been considered to be a potential strategy of FFA sequestration into membrane coated intracellular vesicles (Meyers et al., 2017). It could thus theoretically represent a mechanism to reduce the toxicity of FFA (Borg et al., 2009; Listenberger et al., 2003; Cnop et al., 2001). Oil red O staining results showed that C18:0 incubation obviously induced lipid droplet formation in ZFL cells (Figure S7). However, C20:0 and C22:0 incubation did not cause obvious lipid deposition, indicating that the two SFAs may exist as highly toxic forms of non-triglyceride (Figure S7). It has been reported that the C20:0 and C22:0 mostly exist as the form of FFA. These explained the weakening of the cold resistance ability of ZFL cells with C20:0 or C22:0 incubation.

SFAs in the form of FFAs often have high lipid toxicity. In this study, the long-chain C24:0 incubation did not induce obvious lipid droplet formation. Theoretically, the catabolism of C24:0 should produce a lot of ROS. However, our results showed that the accumulation of C24:0 in ZFL cells under cold stress did not increase the level of oxidative stress but enhanced the cold tolerance. Therefore, we speculate that C24:0 does not provide energy through β-oxidation catabolism and may participate in cold resistance process as a functional substance. Previous reports indicated that C24:0 constitutes nearly 50% of sphingolipids and ceramides in liver (Sassa and Kihara, 2014). It has been reported that C24:0 ceramide could promote the mitochondrial β-oxidation process (Raichur et al., 2014; Mesicek et al., 2010). Our results showed that the expressions of *cers2* and *cers4* (the main enzymes of C24:0 ceramide synthesis) were significantly up-regulated in ZFL cells with C24:0 incubation. Moreover, the level of mitochondrial energy metabolism increased significantly in the C24:0 incubation group. Therefore, the increase of the C24:0 ceramide level promoted mitochondrial β-oxidation and provided the necessary energy for resisting cold stress.

In conclusion, we explored the role of VLC-SFA in the cold resistance of fish. Our results show that zebrafish tend to synthesize abundant C24:0 via *elovl1* genes to resist cold environment. This strategy avoids the apoptosis and oxidative stress induced by C20:0 and C22:0, whereas an increased level of C24:0 ceramide can activate mitochondrial β-oxidation to enhance cold resistance ability. This study could further our understanding of cold resistance mechanisms in fish and provide critical information to protect fish against cold stress.

Limitations of the study

We demonstrated that C24:0 synthetized by *elovl1s* could promote mitochondrial β-oxidation to improve the cold resistance of zebrafish. However, the underlying mechanisms of *elovl1s* activated by cold stress are not clear and deserve further investigations. In addition, the effects of diet C24:0 supplement of just one concentration on the cold resistance of WT zebrafish were studied here. The optimal supplemental concentration of diet C24:0 for zebrafish under cold stress still needs to be confirmed.

STAR★METHODS

Detailed methods are provided in the online version of this paper and include the following:

- KEY RESOURCES TABLE
- RESOURCE AVAILABILITY
  - Lead contact
  - Materials availability
  - Data and code availability
- EXPERIMENTAL MODEL AND SUBJECT DETAILS
  - Animals
  - Animal models
  - ZFL cell line
- METHODS DETAILS
  - Cold stress experiment of ZFL cells
  - ZFL cells incubated with FA solutions
  - Cold stress of $elovl1a^{-/-}$ and $elovl1b^{-/-}$ zebrafish

- ○ Lipidomic analysis
- ○ Oil Red O staining
- ○ Feeding experiment
- ● QUANTIFICATION AND STATISTICAL ANALYSIS

SUPPLEMENTAL INFORMATION

Supplemental information can be found online at https://doi.org/10.1016/j.isci.2021.103409.

AUTHOR CONTRIBUTIONS

S.S. and J.G. designed research; S.S. performed research; S.S. analyzed data; S.S. wrote the paper; J.G. acquired funding; J.G., S.S., and X.C. involved in the discussion; X.C. revised the paper. All authors read and approved the manuscript.

DECLARATION OF INTERESTS

The authors declare no competing interests.

REFERENCES

Beitinger, T.L., Bennett, W.A., and Mccauley, R.W. (2000). Temperature tolerances of North American freshwater fishes exposed to dynamic changes in temperature. Environ. Biol. Fishes 58, 237–275. https://doi.org/10.1023/A:1007676325825.

Ben-David, O., Pewzner-Jung, Y., Brenner, O., Laviad, E.L., Kogot-Levin, A., Weissberg, I., Biton, I.E., Pienik, R., Wang, E., Kelly, S., et al. (2011). Encephalopathy caused by ablation of very long acyl chain ceramide synthesis may be largely due to reduced galactosylceramide levels. J. Biol. Chem. 286, 30022–30033. https://doi.org/10.1074/jbc.M111.261206.

Bhandari, S., Lee, J.N., Kim, Y.I., Nam, I.K., Kim, S.J., Kim, S.J., Kwak, S., Oh, G.S., Kim, H.J., Yoo, H.J., et al. (2016). The fatty acid chain elongase, Elovl1, is required for kidney and swim bladder development during zebrafish embryogenesis. Organogenesis 12, 78–93. https://doi.org/10.1080/15476278.2016.1172164.

Borg, J., Klint, C., Wierup, N., Ström, K., Larsson, S., Sundler, F., Lupi, R., Marchetti, P., Xu, G., Kimmel, A., et al. (2009). Perilipin is present in islets of Langerhans and protects against lipotoxicity when overexpressed in the beta-cell line INS-1. Endocrinology 150, 3049–3057. https://doi.org/10.1210/en.2008-0913.

Brunaldi, K., Huang, N., and Hamilton, J.A. (2010). Fatty acids are rapidly delivered to and extracted from membranes by methyl-beta-cyclodextrin. J. Lipid Res. 51, 120–131. https://doi.org/10.1194/M900200-JLR200.

Buda, C., Dey, I., Balogh, N., Horvath, L.I., Maderspach, K., Juhasz, M., Yeo, Y.K., and Farkas, T. (1994). Structural order of membranes and composition of phospholipids in fish brain cells during thermal acclimatization. Proc. Natl. Acad. Sci. U S A 91, 8234–8238. https://doi.org/10.1073/pnas.91.17.8234.

Busch, F., Mobasheri, A., Shayan, P., Stahlmann, R., and Shakibaei, M. (2012). Sirt-1 is required for the inhibition of apoptosis and inflammatory responses in human tenocytes. J. Biol. Chem. 287, 25770–25781. https://doi.org/10.1074/jbc.M112.355420.

Cnop, M., Hannaert, J.C., Hoorens, A., Eizirik, D.L., and Pipeleers, D.G. (2001). Inverse relationship between cytotoxicity of free fatty acids in pancreatic islet cells and cellular triglyceride accumulation. Diabetes 50, 1771–1777. https://doi.org/10.2337/diabetes.50.8.1771.

Davidovich, P., Kearney, C.J., and Martin, S.J. (2014). Inflammatory outcomes of apoptosis, necrosis and necroptosis. Biol. Chem. 395, 1163–1171. https://doi.org/10.1515/hsz-2014-0164.

Dey, I., Buda, C., Wiik, T., Halver, J.E., and Farkas, T. (1993). Molecular and structural composition of phospholipid membranes in livers of marine and freshwater fish in relation to temperature. Proc. Natl. Acad. Sci. U S A 90, 7498–7502. https://doi.org/10.1073/pnas.90.16.7498.

Donaldson, M., Cooke, S., Patterson, D., and Macdonald, J. (2008). Cold shock and fifish. J. Fish Biol. 73, 1491–1530.

Dyer, W.J., and Bligh, E.G. (1959). A rapid method of total lipid extraction and purification. J. Physiol. Pharmacol. 37, 911–917. https://doi.org/10.1139/o59-099.

Farkas, T. (1980). Metaboliam of fatty acids in fish: III. combined effect of environmental temperature and diet on formation and deposition of fatty acids in the carp, Cyprineus carpio Limaeus. Aquaculture 20, 29–40. https://doi.org/10.1016/0044-8486(80)90059-9.

Green, B.S., and Fisher, R. (2004). Temperature influences swimming speed, growth and larval duration in coral reef fish larvae. J. Exp. Mar. Biol. Ecol. 299, 115–132. https://doi.org/10.1016/j.jembe.2003.09.001.

Hazel, J.R. (1984). Effects of temperature on the structure and metabolism of cell membranes in fish. Am. J. Physiol. 246, R460–R470. https://doi.org/10.1152/ajpregu.1984.246.4.R460.

Heise, K., Puntarulo, S., Nikinmaa, M., Lucassen, M., Pörtner, H.O., and Abele, D. (2006). Oxidative stress and HIF-1 DNA binding during stressful cold exposure and recovery in the North Sea eelpout (Zoarces viviparus). Comp. Biochem. Physiol. A. Mol. Integr. Physiol. 143, 494–503. https://doi.org/10.1016/j.cbpa.2006.01.014.

He, J., Qiang, J., Yang, H., Xu, P., Zhu, Z.X., and Yang, R.Q. (2015). Changes in the fatty acid composition and regulation of antioxidant enzymes and physiology of juvenile genetically improved farmed Tilapia Oreochromis niloticus (L.), subjected to short-term low temperature

stress. J. Therm. Biol. *53*, 90–97. https://doi.org/10.1016/j.jtherbio.2015.08.010.

Hsieh, S.L., Chang, H.T., and Wu, C.H. (2004). Cloning, tissue distribution and hormonal regulation of stearoyl-CoA desaturase in *Tilapia Oreochromis mossambicus*. Aquaculture *230*, 527–546. https://doi.org/10.1016/S0044-8486(03)00408-3.

Hsieh, S.L., Chen, Y.N., and Kuo, C.M. (2003). Physiological responses, desaturase activity, and fatty acid composition in milkfish (*Chanos chanos*) under cold acclimation. Aquaculture *220*, 903–918. https://doi.org/10.1016/S0044-8486(02)00579-3.

Ida, N., Hartmann, T., Pantel, J., Schröder, J., Zerfass, R., Förstl, H., Sandbrink, R., Masters, C.L., and Beyreuther, K. (1996). Analysis of heterogeneous A4 peptides in human cerebrospinal fluid and blood by a newly developed sensitive Western blot assay. J. Biol. Chem. *271*, 22908–22914. https://doi.org/10.1074/jbc.271.37.22908.

Kondoh, K., and Nishida, E. (2007). Regulation of MAP kinases by MAP kinase phosphatases. Biochim. Biophys. Acta *1773*, 1227–1237. https://doi.org/10.1016/j.bbamcr.2006.12.002.

Koopman, R., Schaart, G., and Hesselink, M.K. (2001). Optimisation of oil red O staining permits combination with immunofluorescence and automated quantification of lipids. Histochem. Cell Biol. *116*, 63–68. https://doi.org/10.1007/s004180100297.

Kunau, W.H., Dommes, V., and Schulz, H. (1995). Beta-oxidation of fatty acids in mitochondria, peroxisomes, and bacteria: a century of continued progress. Prog. Lipid Res. *34*, 267–342. https://doi.org/10.1016/0163-7827(95)00011-9.

Kyprianou, T.D., Portner, H.O., Anestis, A., Kostoglou, B., Feidantsis, K., and Michaelidis, B. (2010). Metabolic and molecular stress responses of gilthead seam bream *Sparus aurata* during exposure to low ambient temperature: an analysis of mechanisms underlying the winter syndrome. J. Comp. Physiol. *180*, 1005–1018. https://doi.org/10.1007/s00360-010-0481-y.

Laviad, E.L., Albee, L., Pankova-Kholmyansky, I., Epstein, S., Park, H., Merrill, A.H., and Futerman, A.H. (2008). Characterization of ceramide synthase 2: tissue distribution, substrate specificity, and inhibition by sphingosine 1-phosphate. J. Biol. Chem. *283*, 5677–5684. https://doi.org/10.1074/jbc.M707386200.

Li, J.X., Yang, C., Huang, L., Zeng, K., Cao, X., and Gao, J. (2019). Inefficient ATP synthesis by inhibiting mitochondrial respiration causes lipids to decrease in MSTN-lacking muscles of loach Misgurnus anguillicaudatus. Funct. Integr. Genomics *19*, 889–900. https://doi.org/10.1007/s10142-019-00688-x.

Listenberger, L.L., Han, X., Lewis, S.E., Cases, S., Farese, R.V., Ory, D.S., and Schaffer, J.E. (2003). Triglyceride accumulation protects against fatty acid-induced lipotoxicity. Proc. Natl. Acad. Sci. U S A *100*, 3077–3082. https://doi.org/10.1073/pnas.0630588100.

Lu, D.L., Ma, Q., Sun, S.X., Zhang, H., Chen, L.Q., Zhang, M.L., and Du, Z.Y. (2019a). Reduced oxidative stress increases acute cold stress

tolerance in zebrafish. Comp. Biochem. Physiol. A. Mol. Integr. Physiol. *235*, 166–173. https://doi.org/10.1016/j.cbpa.2019.06.009.

Lu, D.L., Ma, Q., Wang, J., Li, L.Y., Han, S.L., Limbu, S.M., Li, D.L., Chen, L.Q., Zhang, M.L., and Du, Z.Y. (2019b). Fasting enhances cold resistance in fish through stimulating lipid catabolism and autophagy. J. Physiol. *597*, 1585–1603. https://doi.org/10.1113/JP277091.

Mesicek, J., Lee, H., Feldman, T., Jiang, X., Skobeleva, A., Berdyshev, E.V., Haimovitz-Friedman, A., Fuks, Z., and Kolesnick, R. (2010). Ceramide synthases 2, 5, and 6 confer distinct roles in radiation-induced apoptosis in HeLa cells. Cell Signal. *22*, 1300–1307. https://doi.org/10.1016/j.cellsig.2010.04.006.

Meyers, A., Weiskittel, T.M., and Dalhaimer, P. (2017). Lipid droplets: formation to Breakdown. Lipids *52*, 465–475. https://doi.org/10.1007/s11745-017-4263-0.

Moreno-Mateos, M.A., Vejnar, C.E., Beaudoin, J.D., Fernandez, J.P., Mis, E.K., Khokha, M.K., and Giraldez, A.J. (2015). CRISPRscan: designing highly efficient sgRNAs for CRISPR-Cas9 targeting in *vivo*. Nat. Methods *12*, 982–988. https://doi.org/10.1038/nmeth.3543.

Ohno, Y., Suto, S., Yamanaka, M., Mizutani, Y., Mitsutake, S., Igarashi, Y., Sassa, T., and Kihara, A. (2010). ELOVL1 production of C24 acyl-CoAs is linked to C24 sphingolipid synthesis. Proc. Natl. Acad. Sci. U S A *107*, 18439–18444. https://doi.org/10.1073/pnas.1005572107.

Overstreet, R.M. (1974). An estuarine low temperature fish kill in Mississippi, with remarks on restricted necropsies. Gulf Res. Rep. *4*, 328–350. https://doi.org/10.18785/grr.0403.02.

Patterson, K.I., Brummer, T., O'Brien, P.M., and Daly, R.J. (2009). Dual-specificity phosphatases: critical regulators with diverse cellular targets. Biochem. J. *418*, 475–489. https://doi.org/10.1042/bj20082234.

Plötz, T., von Hanstein, A.S., Krümmel, B., Laporte, A., Mehmeti, I., and Lenzen, S. (2019). Structure-toxicity relationships of saturated and unsaturated free fatty acids for elucidating the lipotoxic effects in human EndoC-βH1 beta-cells. Biochim. Biophys. Acta Mol. Basis Dis. *1865*, 165525. https://doi.org/10.1016/j.bbadis.2019.08.001.

Raichur, S., Wang, S.T., Chan, P.W., Li, Y., Ching, J., Chaurasia, B., Dogra, S., Öhman, M.K., Takeda, K., Sugii, S., et al. (2014). CerS2 haploinsufficiency inhibits β-oxidation and confers susceptibility to diet-induced steatohepatitis and insulin resistance. Cell Metab. *20*, 687–695. https://doi.org/10.1016/j.cmet.2014.09.015.

Rocha, D.M., Caldas, A.P., Oliveira, L.L., Bressan, J., and Hermsdorff, H.H. (2016). Saturated fatty acids trigger TLR4-mediated inflammatory response. Atherosclerosis *244*, 211–215. https://doi.org/10.1016/j.atherosclerosis.2015.11.015.

Sabnam, S., and Pal, A. (2019). Relevance of Erk1/2-PI3K/Akt signaling pathway in CEES-induced oxidative stress regulates inflammation and apoptosis in keratinocytes. Cell. Biol. Toxicol. *35*, 541–564. https://doi.org/10.1007/s10565-019-09467-7.

Sassa, T., and Kihara, A. (2014). Metabolism of very long-chain Fatty acids: genes and pathophysiology. Biomol. Ther. (Seoul) *22*, 83–92. https://doi.org/10.4062/biomolther.2014.017.

Schulz, H. (1994). An overview of the pathways for the beta-oxidation of polyunsaturated fatty acids. World Rev. Nutr. Diet *75*, 18–21. https://doi.org/10.1159/000423545.

Šrámek, J., Němcová-Fürstová, V., Pavlíková, N., and Kovář, J. (2017). Effect of saturated stearic acid on MAP kinase and ER stress signaling pathways during apoptosis Induction in human pancreatic β-cells is inhibited by unsaturated oleic acid. Int. J. Mol. Sci. *18*, 2313. https://doi.org/10.3390/ijms18112313.

Sun, J., Chen, L., Jiang, P., Duan, B., Wang, R., Xu, J., Liu, W., Xu, Y., Xie, Z., Feng, F., and Qu, W. (2020a). Phenylethanoid glycosides of Callicarpa kwangtungensis Chun exert cardioprotective effect by weakening Na+-K+-ATPase/Src/ERK1/2 pathway and inhibiting apoptosis mediated by oxidative stress and inflammation. J. Ethnopharmacol. *258*, 112881. https://doi.org/10.1016/j.jep.2020.112881.

Sun, S., Ren, T., Li, X., Cao, X., and Gao, J. (2020b). Polyunsaturated fatty acids synthesized by freshwater fish: a new insight to the roles of *elovl2* and *elovl5* in *vivo*. Biochem. Biophys. Res. Commun. *532*, 414–419. https://doi.org/10.1016/j.bbrc.2020.08.074.

Tamura, K., Makino, A., Hullin-Matsuda, F., Kobayashi, T., Furihata, M., Chung, S., Ashida, S., Miki, T., Fujioka, T., Shuin, T., et al. (2009). Novel lipogenic enzyme ELOVL7 is involved in prostate cancer growth through saturated long-chain fatty acid metabolism. Cancer Res. *69*, 8133–8140. https://doi.org/10.1158/0008-5472.CAN-09-0775.

Tamer, F., Ulug, E., Akyol, A., and Nergiz-Unal, R. (2020). The potential efficacy of dietary fatty acids and fructose induced inflammation and oxidative stress on the insulin signaling and fat accumulation in mice. Food Chem. Toxicol. *135*, 110914. https://doi.org/10.1016/j.fct.2019.110914.

Tseng, Y.C., Chen, R.D., Lucassen, M., Schmidt, M.M., Dringen, R., Abele, D., and Hwang, P.P. (2011). Exploring uncoupling proteins and antioxidant mechanisms under acute cold exposure in brains of fish. PLoS ONE *6*, e18180. https://doi.org/10.1371/journal.pone.0018180.

Turpin, S.M., Nicholls, H.T., Willmes, D.M., Mourier, A., Brodesser, S., Wunderlich, C.M., Mauer, J., Xu, E., Hammerschmidt, P., Brönneke, H.S., et al. (2014). Obesity-induced CerS6-dependent C16:0 ceramide production promotes weight gain and glucose intolerance. Cell. Metab. *20*, 678–686. https://doi.org/10.1016/j.cmet.2014.08.002.

Tvrdik, P., Asadi, A., and Kozak, L.P. (1997). Cig30, a mouse member of a novel membrane protein gene family, is involved in the recruitment of brown adipose tissue. J. Biol. Chem. *272*, 31738–31746. https://doi.org/10.1074/jbc.272.50.31738.

Vinagre, C., Madeira, D., Narciso, L., Cabral, H.N., and Diniz, M. (2012). Effect of temperature on oxidative stress in fish: lipid peroxidation and catalase activity in the muscle of juvenile seabass.

Dicentrarchus Labrax Ecol. Indic *23*, 274–279. https://doi.org/10.1016/j.ecolind.2012.04.009.

Vogel, R.A., Corretti, M.C., and Plotnick, G.D. (1997). Effect of a single high-fat meal on endothelial function in healthy subjects. Am. J. Cardiol. *79*, 350–354. https://doi.org/10.1016/s0002-9149(96)00760-6.

Wu, C.L., Lin, T.H., Chang, T.L., Sun, H.W., Hui, C.F., and Wu, J.L. (2011). Zebrafish HSC70

promoter to express carp muscle-specific creatine kinase for acclimation under cold condition. Transgenic Res. *20*, 1217–1226. https://doi.org/10.1007/s11248-011-9488-8.

Zhang, Y.F., Wang, L.W., Cao, X.J., and Gao, J. (2018). Cloning and characteristic analysis of *elovl1* genes from loach (*Misgurnus anguillicaudatus*) and its role in adaptation to cold temperature. J. Huazhong Agric. Univ. *37*,

102–111. https://doi.org/10.13300/j.cnki.hnlkxb.2018.04.014.

Zhao, Y., Cao, X., Fu, L., and Gao, J. (2020). n-3 PUFA reduction caused by *fabp2* deletion interferes with triacylglycerol metabolism and cholesterolhomeostasis in fish. Appl. Microbiol. *104*, 2149–2161. https://doi.org/10.1007/s00253-020-10366-9.

STAR★METHODS

KEY RESOURCES TABLE

REAGENT or RESOURCE	SOURCE	IDENTIFIER
Antibodies		
Anti-Elovl1a	This paper	N/A
Anti-Elovl1b	This paper	N/A
Anti-Erk1/2	This paper	N/A
Anti-Gapdh	Servicebio	Cat#GB11002
FITC-Goat anti-Rabbit IgG (H+L)	Biosharp	Cat#BL033A
Chemicals, peptides, and recombinant proteins		
C14:0 FA	Aladdin	CAS#544-63-8
C16:0 FA	Aladdin	CAS#57-10-3
C18:0 FA	Aladdin	CAS#57-11-4
C20:0 FA	Cayman	CAS#506-30-9
C22:0 FA	Cayman	CAS#112-85-6
C24:0 FA	Cayman	CAS#557-59-5
C16:1 FA	Cayman	CAS#17004-51-2
C18:1 FA	Aladdin	CAS#112-80-1
C20:1 FA	Cayman	CAS#29204-02-2
C22:1 FA	Cayman	CAS#112-86-7
MβCD	Macklin	CAS#128446-36-6
MS-222	Sigma -Aldrich	CAS#886-86-2
Vitamin E	NacalaiTesque	CAS#10191-41-0
butylated hydroxytoluene	Aladdin	CAS#128-37-0
Critical commercial assays		
CAT assay kit	Nanjing Jiancheng Bioengineering Institute	Cat#A007-1-1
MDA assay kit	Nanjing Jiancheng Bioengineering Institute	Cat#A003-1-2
Annexin V-FITC/PI Apoptosis Detection Kit	Yisheng	Cat#40302ES50
Deposited data		
Lipomics data	This paper	MetaboLights: MTBLS3355
Experimental models: Cell lines		
ZFL: zebrafish liver cell	China Zebrafish Resource Center	Cell2
Experimental models: Organisms/strains		
Zebrafish (AB)	China Zebrafish Resource Center	CZ1
Oligonucleotides		
Primers	This paper	Table S1
Software and algorithms		
GraphPad Prism 6	GraphPad Software Inc.,	N/A
IBM SPSS statistics 22 software	SPSS Inc.,	N/A
MetaboAnalyst 5.0		https://www.metaboanalyst.ca/

RESOURCE AVAILABILITY

Lead contact

Further information and requests for resources and reagents should be directed to and will be fulfilled by the lead contact, Jian Gao (gaojian@mail.hzau.edu.cn).

Materials availability

Zebrafish lines generated in this study are available from the lead contact upon reasonable request.

Data and code availability

- The lipidomics data are available in the MetaboLights database, and accession numbers are listed in the Key resources table. All data reported in this paper will be shared by the lead contact upon request.

- This paper does not report original code.

- Any additional information required to reanalyze the data reported in this paper is available from the lead contact upon request.

EXPERIMENTAL MODEL AND SUBJECT DETAILS

Animals

This study was conducted in strict accordance with the recommendations in the guide for the care and use of laboratory animals of Huazhong Agricultural University. This study was approved by the Committee on the Ethics of Animal Experiments of Huazhong Agricultural University (HZAUFI-2021-0024). To minimize suffering, zebrafish were killed after anesthesia with MS-222.

Zebrafish (AB strain, obtained from the Institute of Hydrobiology, Chinese Academy of Sciences, China Zebrafish Resource Center, Wuhan, China) were raised in 28°C circulating water with the photoperiod and dark cycle of 14h and 10h, respectively, and fed three times daily with freshly hatched brine shrimp. Two-month-old zebrafish of both sexes were used in this study.

Animal models

Sexually mature WT zebrafish were used for artificial propagation. The zebrafish *elovl1a* and *elovl1b* knockout model were generated by using the CRISPR/Cas9 technology. The DNA sequences of zebrafish *elovl1a* and *elovl1b* were obtained from NCBI. *In vitro* transcription of Cas9 RNA and gRNA were based on the standards of the relevant research (Moreno-Mateos et al., 2015). Detailed construction methods were performed as previously described (Zhao et al., 2020). The genomic DNA was isolated from 6 randomly selected fertilized embryos. Next, the target genome region was amplified and sequenced. Once the mutation was confirmed in injected embryos, the remaining ones were raised to adulthood. The F0 founders carrying mosaic mutations were identified by heteroduplex motility assay. The mutant F0 was then genetically outcrossed with WT zebrafish to produce F1 generation. Two months later, the heterozygous F1 generation with the same mutation sequences, confirmed by sequencing the genomic DNA from the cut tail fin, was self-crossed. About a quarter of the F2 generation obtained were homozygous mutants. The F3 individuals of two-month-old produced by self-crossing F2 homozygous mutants were used in this study. By crossing the *elovl1a*$^{-/-}$ zebrafish with the *elovl1b*$^{-/-}$ zebrafish, we obtained double heterozygous offspring. The double heterozygous zebrafish were then self-crossed to produce the DKO zebrafish.

ZFL cell line

The ZFL cells (obtained from the China Zebrafish Resource Center, Wuhan, China) were maintained in modified limit dilution factor (LDF) medium (50% Leibowitz-15, 35% Dulbecco's Modified Essential Medium, 15% HAM's F12, 15 mM HEPES, 0.15 g/L NaHCO$_3$ and 10 μg/mL bovine insulin) supplemented with 5% (v/v) fetal bovine serum (FBS, Gibco), and 2% antibiotic (100 U/mL penicillin, 100 μg/mL streptomycin) and kept at 28°C in a 0.5% CO$_2$ incubator.

METHODS DETAILS

Cold stress experiment of ZFL cells

To explore the changes of fatty acid compositions in ZFL cells under cold stress, three dishes of the cells were transported to an incubator at 10°C. The other three dishes of the cells were maintained at 28°C as the control. The total RNA was extracted for real-time quantitative PCR (qPCR) after 24 h of cold stress, and the fatty acid composition analysis and western blotting analysis were carried out after 48 h of cold stress.

For cold stress experiment of ZFL cells incubated with SFA, 8 groups of the cells were treated with equal volume of dissolvant (as control), C18:0 (5μM), C20:0 (5μM), C22:0 (5μM), C24:0 (5μM), C20:0 (5μM)+VE (100μM), C22:0 (5μM)+VE (100μM), C24:0 (5μM)+VE (100μM), respectively. After maintained at 28°C for 12 h, the ZFL cells were transported to an incubator at 10°C. The apoptosis detection was conducted after 24 h of cold stress. qPCR and western blotting analysis were performed after 48 h of cold stress. We used 5μM SFA to challenge ZFL cells because it was a suitable lethal concentration for the cells based on our preliminary results.

Fatty acid composition analysis.   Total lipid was extracted by using the Bligh and Dyer procedure as previously described (Dyer and Bligh, 1959). Then, the total lipid was methylated for 1.5h at 85°C with 3mL methylation reagent containing 1% H_2SO_4, 99% methylation and 0.005% butylated hydroxytoluene to produce fatty acid methyleters. The fatty acid compositions were determined by using a gas chromatography (Shimadzu emit Co., Ltd, Tokyo, Japan) according to our previous methods (Sun et al., 2020a, 2020b).

RNA extraction and qPCR assays.   Total RNA was extracted by using RNA isoPius following the manufacturer's instructions (TaKaRa, Japan). Detailed methods were performed as previously described (Zhao et al., 2020). The $2^{-\Delta\Delta CT}$ method was used to analyze the expression levels of the target genes with beta-actin (*β-actin*) and 18S ribosomal RNA (*18s rRNA*) used as reference genes. The primer sequences for qPCR are listed in Table S1.

Western blotting analysis.   For total protein isolation, cells/liver tissues were harvested and lysed on ice in RIPA buffer (Boster Biological Technology, Wuhan, China). After centrifugation at 12,000 rpm for 15 min, the supernatant was collected. Protein concentration was measured by the bicinchoninic acid protein assay kit (Beyotime, Haimen, China). The protein expression assays were determined according to the method described by Ida et al. (1996). Specific primary antibodies including Elovl1a (Rabbit), Elovl1b and Erk1/2 antibody were prepared in Frdbio Co., Ltd (Wuhan, China). The corresponding peptide sequences were Elovl1a (293-315aa) and Elovl1b (302-320aa). The recombinant Erk1/2 protein (Full length) was used to prepare polyclonal antibody. Immunoreactive bands were visualized via Odyssey Infrared Fluorescent Western Blots Imaging System (Li-Cor Bioscience, Lincoln, USA) or enhanced chemiluminescence (Cell Signaling Technology).

Apoptosis detection.   For apoptosis detection, Annexin V-FITC/PI Apoptosis Detection Kit (YiSheng, Shanghai, China) was used to detect cell apoptosis according to the manufacturer's instructions. Briefly, cells were treated with indicated treatments, collected, and resuspended in 1× binding buffer with annexin V-FITC (2.5 μL per well) and propidium iodide (PI; 5 μL per well) and incubated in the dark for about 15 min, and then cell suspension was analyzed by flow cytometry.

ZFL cells incubated with FA solutions

The detailed methods of preparation of FA solutions were performed as previously described with some modifications (Brunaldi et al., 2010). Briefly, aliquots (500 μL) of a methyl-β-cyclodextrin (MβCD) solution in water were added to a microcentrifuge tube containing one of the pure SFA: C14:0, C16:0, C18:0, C20:0, C22:0 and C24:0, followed by incubation at 70°C for 30 min and sonication for 5 min to obtain the stock solution at 2 mM. A stock solution of MβCD alone was made in water at 100 mM. For MUFA treatment, the stock solutions of C16:1, C18:1, C20:1, C22:1 (2 mM) were prepared in ethanol. All FAs used in this study were purchase from Aladdin Co., Ltd, China and Cayman Chemical Company, USA. The ZFL cells were incubated with either 50 μM SFA or MUFA at 28°C for 24 h (in triplicate per treatment). Then, expression analysis of *elovl1a* and *elovl1b* and Oil red O staining were performed.

Cold stress of *elovl1a*$^{-/-}$ and *elovl1b*$^{-/-}$ zebrafish

Cold stress trial.   Before the cold stress experiment, WT, *elovl1a*$^{-/-}$ and *elovl1b*$^{-/-}$ zebrafish were starved for 24 h at 28°C to avoid oxidative stress caused by feeding (Lu et al., 2019a).

A total of 60 WT, 60 *elovl1a*$^{-/-}$ and 60 *elovl1b*$^{-/-}$ zebrafish with uniform-size (0.16 ± 0.01 g) were used. They were then immediately subjected to cold stress by transferring them to aseptic and transparent 8 L tanks containing 10°C water. The fish was considered dead when it stopped any movement and activities for at least 1 h. Dead fish were collected and counted every 12 h. The survival rate was counted until all *elovl1a*$^{-/-}$

zebrafish died (this group was the earliest group with all individuals died). The cold stress experiment was again performed with new fish for sampling. After 5 d of cold stress (one of the groups had a mortality rate of more than 50%), livers from each group were collected for staining, qPCR analysis, CAT activity assay, MDA level assay and western blotting analysis.

Activities of CAT and the MDA level. CAT activity and MDA level of zebrafish liver were measured by using the CAT assay kit and MDA assay kit (Nanjing Jiancheng Bioengineering Institute, Nanjing, China) according to the instruction manual, respectively.

Lipidomic analysis

Lipid was extracted from fresh livers (∼20 mg) from WT, *elovl1a*$^{-/-}$ and *elovl1b*$^{-/-}$ zebrafish. Lipidomics were analyzed by the method described previously (Li et al., 2019). The liquid chromatography/tandem mass spectrometry (Shimadzu Emit Co., Ltd, Tokyo, Japan) was applied. A Kromasil 100-2.5-C18 column (2.1 mm × 100 mm; 2.5 μm, part number: MH2CLD10) was used as a reversed phase to separate the lipids. Mobile phase A was ultrapure water with 5 mmol/L ammonium acetate. The mobile phase B was methanol with 5 mmol/L ammonium acetate. The HPLC system was coupled to a TRIPLE QUADTM 3500 mass spectrometer (AB Sciex, USA) via electrospray ionization (ESI) source and was ran in negative ion mode under multiple reaction monitoring (MRM), and the LC/MS spectra were obtained by using enhanced production scan mode at a scan speed of 1000 Da/s. Next, the data obtained were extracted and preprocessed with lipid view software (AB Sciex, Redwood City, CA, USA).

Oil Red O staining

For the visualization of the Oil Red O staining, ZFL cells were grown on glass cover slips. The cells were treated with C18-C24 SFA (50 μM) for 24h at 28°C. Then the ZFL cells climbing sheets were fixed in cold 10% buffered formalin for 20 min, and stained by using a standard Oil Red O method (Koopman et al., 2001) for light microscopy observation.

Feeding experiment

The experiment diets were prepared by using commercial feed (35% crude protein, 3% crude lipid, 10% ash and 4% fiber, PIKE Biotechnology Co., Ltd). Finely ground feed (50 g) was supplemented with 200 mg of each of the following SFA: C18:0, C20:0, C22:0, C24:0, by mixing the feed particles with a solution of fatty acids in hexane. After air drying, the experimental diets were stored at −20°C until further use. 250 WT zebrafish were divided equally into five groups and fed at a fixed ration (20mg/fish/day) with standard diet (control) or SFA diets for 2 weeks. Then 20 zebrafish in each group were selected for cold stress experiment. The survival rate was counted until all zebrafish from one of the groups died. The cold stress experiment was again performed with new fish for sampling. After 6 d of cold stress, livers from each group were collected for MDA level measurement, CAT activity assay, qPCR analysis, and western blotting analysis.

QUANTIFICATION AND STATISTICAL ANALYSIS

For statistical analysis of lipidomic data, all data were then log2 transformed to ensure that they were normally distributed. A Fisher test was used to assess whether missing values were missing at random or if there was an underlying bias. Lipid species were excluded if they were detectable in less than 50% of the samples per group. A standard two-sided, unpaired *T* test assuming unequal variances was used to test for significantly different abundances in the conditions. The lipidomic data were relatively quantitative value. The lipidomic data sets were imported in MetaboAnalyst 5.0, in which the data were analyzed by heatmap visualization.

Except the lipidomic data, other data were expressed as the means ± SD. For two-group comparison of data, *T*-test was performed. For multi-group comparison of data, one-factor ANOVA with Tukey's post hoc tests were carried out. All statistical analyses were performed by using IBM SPSS statistics 22 software (SPSS Inc., USA), and $p < 0.05$ was considered statistically significant. The number of replicates for each experiment was indicated in the figure legends.